AIMS Mathematics, 8(2): 3699–3729.
DOI: 10.3934/math.2023185
Received: 01 July 2022
Revised: 05 November 2022
Accepted: 10 November 2022
Published: 25 November 2022

http://www.aimspress.com/journal/Math

Research article

On the comparative performance of fourth order Runge-Kutta and the Galerkin-Petrov time discretization methods for solving nonlinear ordinary differential equations with application to some mathematical models in epidemiology

Attaullah[1], Mansour F. Yassen[2,3], Sultan Alyobi[4], Fuad S. Al-Duais[5,6] and Wajaree Weera[7,*]

[1] Department of Mathematics & Statistics, Bacha Khan University, Charsadda 24461, Pakistan
[2] Department of Mathematics, College of Science and Humanities in Al-Aflaj, Prince Sattam Bin Abdulaziz University, Al-Aflaj 11912, Saudi Arabia
[3] Department of Mathematics, Faculty of Science, Damietta University, New Damietta 34517 Damietta, Egypt
[4] King Abdulaziz University, College of Science & Arts, Department of Mathematics, Rabigh, Saudi Arabia
[5] Department of Mathematics, College of Science and Humanities in Al-Aflaj, Prince Sattam bin Abdulaziz University, Al-Kharj, Al-Aflaj 11942, Saudi Arabia
[6] Administration Department, Administrative Science College, Thamar University, Thamar, Yemen
[7] Department of Mathematics, Faculty of Science, Khon Kaen University, Khon Kaen, 40002, Thailand

* **Correspondence:** Email: wajawe@kku.ac.th.

Abstract: Anti-viral medication is comparably incredibly beneficial for individuals who are infected with numerous viruses. Mathematical modeling is crucial for comprehending the various relationships involving viruses, immune responses and health in general. This study concerns the implementation of a *continuous* Galerkin-Petrov time discretization scheme with mathematical models that consist of nonlinear ordinary differential equations for the hepatitis B virus, the Chen system and HIV infection. For the Galerkin scheme, we have two unknowns on each time interval which have to be computed by solving a 2×2 block system. The proposed method is accurate to order 3 in the whole time interval and shows even super convergence of order 4 in the discrete time points. The study presents the accurate solutions achieved by means of the aforementioned schemes, presented numerically and graphically. Further, we implemented the classical fourth-order Runge-Kutta scheme accurately and performed various numerical tests for assessing the efficiency and computational cost (in terms of time) of the suggested schemes. The performances of the fourth order Runge-Kutta and the Galerkin-Petrov time discretization approaches for solving nonlinear ordinary differential equations were compared, with

applications towards certain mathematical models in epidemiology. Several simulations were carried out with varying time step sizes, and the efficiency of the Galerkin and Runge Kutta schemes was evaluated at various time points. A detailed analysis of the outcomes obtained by the Galerkin scheme and the Runge-Kutta technique indicates that the results presented are in excellent agreement with each other despite having distinct computational costs in terms of time. It is observed that the Galerkin scheme is noticeably slower and requires more time in comparison to the Runge Kutta scheme. The numerical computations demonstrate that the Galerkin scheme provides highly precise solutions at relatively large time step sizes as compared to the Runge-Kutta scheme.

Keywords: HBV model; the cGP(2)-method; RK4-method; numerical comparison; efficiency of methods
Mathematics Subject Classification: 34A12, 34K28

1. Introduction

Epidemiology is the foundation of public health and is defined as the study of the distribution and determinants of diseases or disorders within groups of people, and the development of knowledge on how to prevent and control them. Epidemiological research helps us understand not only who has a disorder or disease but why and how it was brought to this individual or region. Nowadays, epidemiologists use the insights gathered in their research to determine how illness within a population affects our society and systems on a larger scale, and, in turn, they provide recommendations for interventions. The hepatitis B virus (HBV) became widespread, and epidemiologists around the world worked to control the spread. The epidemiology of HBV infection is diverse, with population prevalence, age and mode of acquisition and likelihood of progression to chronic infection mutually interdependent. Hepatitis B is a life-threatening liver disease caused by the HBV [1, 2], which has a circular genome made of partly double-stranded DNA and is difficult to eradicate after infection due to the development of cccDNA [1, 3]. HBV may induce both acute sickness and chronic liver infection, with sustained blood levels of HBV surface antigen (HBsAg), IgG anti-core antigen (anti-HBc), and HBV DNA [3]. Chronic infection may progress to cirrhosis or liver cancer [4]. According to the World Health Organization, around 2 billion individuals worldwide have been infected with the virus, with approximately 350 million having HBV. Each year, HBV causes approximately 600,000 fatalities. Hepatitis B is prevalent in China, with an estimated 93 million people afflicted [5]. Due to the high risk of infection and the high number of fatalities associated with HBV, it is critical to improve our knowledge of the dynamics of HBV illness. HBV is spread by contact with the blood or other bodily fluids of the infected individuals [2]. Generally, the average age at which people get affected is influenced by the population's infection incidence [5]. Transmission from mother to baby occurs throughout pregnancy, delivery and the postpartum period. Vaccination, including passive immunoprophylaxis and postnatal proactive vaccination, is effective in protecting infants against contracting HBV during labor and delivery and in the postnatal period, but it cannot halt HBV prenatal infection [6–11]. Mathematical models may assist us in gaining insight into disease transmission, evaluating the success of different preventative methods, and ultimately bringing the illness under control. Mathematical modeling of a dynamical system is an interesting

study area that has grabbed the interest of a majority of researchers. Dynamical systems have a wide range of applications, including population growth models, biomedical research, biological systems, and engineering. Aniji et al. [12] established a mathematical model of hepatitis B virus infection for antiviral treatment that depicts the probable interaction between HBV and target liver cells. Zada et al. [13] evaluated and analyzed the hepatitis B epidemic model with optimal control. Zhao et al. [14] designed a mathematical model of hepatitis B viral transmission and addressed its potential use in China's immunization plan. Means et al. [15] explored the Hepatitis B Virus's geographical impacts and potential function. Khatun et al. [16] explored viral dynamics, which aids in the understanding of the dynamics of HIV, hepatitis B virus (HCB), hepatitis C virus (HCV), and many other viruses. Additionally, they explored the hepatitis B virus model with Cytotoxic T Lymphocyte (CTL) immunological responses. Zhang et al. [17] developed a mathematical model to explain how hepatitis B spreads. The stability of equilibria and illness persistence are investigated. The study demonstrated that the model's dynamics are entirely determined by the basic reproductive number. Khan et al. [18] reported a detailed analysis of the Hepatitis B model using the Caputo-Fabrizio fractional derivative. The required findings are obtained by establishing the criteria for the existence and uniqueness of the solution to the considered model using fixed point theory. The *continuous* Galerkin-Petrov (cGP) discretization scheme is a very popular and powerful approach to handling complex dynamical systems. Numerous researchers addressed so many interesting properties and some feasible practical applications of the proposed scheme's implementation. Attaullah and Sohaib [19] employed a *continuous* Galerkin-Petrov (cGP) discretization scheme with a mathematical model of Human Immunodeficiency Virus (HIV) infection, which contained a system of nonlinear differential equations. They validated the results of the proposed scheme in comparison to other traditional schemes. Hussain et al. [20] utilized the Galerkin method with the Chen model and performed a comparison between the findings of the Galerkin technique and the fourth-order Runge-Kutta (RK4) method for the presented problem. They concluded that the Galerkin scheme achieved more accurate results at larger time step sizes than the RK4 method. Hussain [21] implemented a novel class of higher-order Galerkin temporal discretization techniques for non-stationary incompressible flow problems. Attaullah et al. [22] implemented the Galerkin time discretization scheme for the transmission dynamics of HIV infection with nonlinear supply rate and discussed the impact of different physical parameters on the population dynamics of healthy/infected cells and virus particles. Schieweck [23] described A-stable discontinuous Galerkin-Petrov time discretization of higher-order. For the heat equation, higher-order Galerkin temporal discretizations and fast multigrid solvers were used by Hussain et al. [24]. For the non-stationary Stokes equations, Hussain et al. [25] demonstrated an accurate and efficient higher-order Galerkin time-stepping approach. For nonlinear systems of ordinary differential equations, higher-order variational time discretizations were utilized by Matthies and Schieweck [25]. Attaullah et al. [26] numerically simulated the HIV model using a Galerkin approach. To validate the numerical results, a detailed evaluation of the outcomes achieved by the Galerkin scheme is contrasted with the findings of the RK4 technique. Various simulations were carried out to evaluate the findings of the Galerkin and RK4 approach, demonstrating the credibility of the cGP(2) technique. The comparison analysis and graphical plots illustrate that the Galerkin scheme is more appropriate than the RK4 method for achieving high accuracy at larger step sizes. For the approximate solution of the HIV model with a variable source term and full logistic proliferation, Attaullah et al. [27] implemented the Galerkin-technique and compared the results with the findings

of the RK4 method. Khan et al. [28] described a mathematical model for the transmission dynamics of acute and chronic hepatitis B and developed an optimal control method for hepatitis B spread in a community. Numerous models of HBV transmission dynamics have been developed to examine the effect of preventative and control methods such as vaccination, antiviral therapy and the incidence rate [29–32]. These models have provided valuable insight into the effectiveness of different control strategies. However, the majority of these models have been studied primarily analytically. The mathematical model proposed in the paper is the extension of the model presented by Khan et al. [28] by including a non-linear saturated incidence rate [32] and investigated numerically. We carry out a comprehensive investigation of the various influence of several clinical parameters. The main contributions are as follows:

1. Implemented Galerkin scheme and the RK4 scheme correctly to the HBV model and presented the solutions numerically and graphically.
2. The significant effects of the various physical parameters are visualized accurately.
3. To authenticate the validity and reliability of the suggested scheme, employed the proposed schemes to other mathematical models (Chen System and the HIV infection model) existing in the literature.
4. The comparative study is performed to validate the accuracy (adopting various step sizes) and computational cost (in terms of time) of Galerkin and RK4-scheme.
5. Finally, invoked the methods to the problem having an exact solution and confirm the accuracy and time consuming with different step sizes.

2. The mathematical model of Hepatitis B Virus

The mathematical model addressed here is as follows:

$$\frac{d\tilde{S}}{dt} = e - \frac{\eta\tilde{S}(t)\tilde{I}_2(t)}{1+\xi_1\tilde{I}_2} - (\phi_0+\lambda)\tilde{S}(t), \tag{2.1}$$

$$\frac{d\tilde{I}_1}{dt} = \frac{\eta\tilde{S}(t)\tilde{I}_2(t)}{1+\xi_1\tilde{I}_2} - (\phi_0+\xi+\psi_1)\tilde{I}_1(t), \tag{2.2}$$

$$\frac{d\tilde{I}_2}{dt} = \xi\tilde{I}_1(t) - (\phi_0+\phi_1+\psi_2)\tilde{I}_2(t), \tag{2.3}$$

$$\frac{d\tilde{R}}{dt} = \psi_1\tilde{I}_1(t) + \psi_2\tilde{I}_2(t) + \lambda\tilde{S}(t) - \phi_0\tilde{R}(t). \tag{2.4}$$

In the this model the population $\tilde{T}(t)$ is divided into four compartments: susceptible individuals $\tilde{S}(t)$, infected individuals $\tilde{I}_1(t)$, infected individuals with chronic hepatitis B (CHB), $\tilde{I}_2(t)$ and recovered individuals $\tilde{R}(t)$. The initial conditions and the detailed information of all parameters included in the model are presented in Table 1.

Table 1. The description of variables, parameters, with their values involved in model (unit=day^{-1}mm^{-3}) [28].

Variable	Explanation	Value
$\tilde{S}(0)$	Susceptible individuals	100
$\tilde{I}_1(0)$	Infected individuals with acute HBV	40
$\tilde{I}_2(0)$	Infected individuals with chronic HBV	20
$\tilde{R}(0)$	Recovered individuals	5
e	Birth rate	0.4
η	The rate of moving from susceptible to infected with acute hepatitis B	0.005
ξ	The rate of moving from the acute stage to infected with chronic hepatitis B.	0.01
ψ_1	The rate of rehabilitation from the acute stage to the recovered stage	0.05
ψ_2	The rate of rehabilitation from the chronic stage to the recovered stage	0.06
ϕ_0	Natural death rate	0.003
ϕ_1	Death rate happening due to hepatitis B	0.002
λ	Vaccination rate of Hepatitis B	0.02
ξ_1	Saturation constant	0.004

3. The numerical schemes

3.1. The continuous Galerkin-Petrov method

The Galerkin technique has been widely employed in recent years to handle a wide range of nonlinear problems in science and engineering, such as [23–25, 33–35, 37, 43, 44]. In this paper, we are using this approach for the models discussed in [19, 20, 27, 28, 38]. The system of ODEs for the considered model can be written as follows:
Find $\tilde{\mathbf{u}} : [0, t_{max}] \to \mathbf{V} = \mathbb{R}^d$ *such that*

$$\begin{aligned} &d_t\tilde{\mathbf{u}}(t) = F(t, \tilde{\mathbf{u}}(t)) \quad \forall\, t \in I, \\ &\tilde{\mathbf{u}}(0) = \tilde{\mathbf{u}}_0, \end{aligned} \tag{3.1}$$

where d_t shows the derivative of $\tilde{\mathbf{u}}(t)$ w.r.t. time, I=[0, T] is the time interval, $\tilde{\mathbf{u}}(t) = (\tilde{u}_1(t),\ \tilde{u}_2(t),\ \tilde{u}_3(t)) \in V \Rightarrow \tilde{\mathbf{u}}(0) = (\tilde{u}_1(0), \tilde{u}_2(0), \tilde{u}_3(0)) \in V$ are the initial values of $\tilde{\mathbf{u}}(t)$ at time $t = 0$. We also assume that $(\tilde{u}_1(t),\ \tilde{u}_2(t),\ \tilde{u}_3(t)) = (T(t),\ I(t),\ V(t))$, which implies that $(\tilde{u}_1(0),\ \tilde{u}_2(0),\ \tilde{u}_3(0)) = (T(0), I(0), V(0))$. The function $F = (f_1, f_2, f_3)$ is nonlinear and is defined as F $: I \times K \to K$.
The *weak formulation* of Problem (3.1) is: Find $\tilde{u} \in$ X such that $\tilde{\mathbf{u}}(0) = \tilde{\mathbf{u}}_0$ and

$$\int_I \langle d_t\tilde{\mathbf{u}}(t), v(t)\rangle\, dt = \int_I \langle F(t, \tilde{\mathbf{u}}(t), v(t))\rangle\, dt \quad for\ all\ v \in Y, \tag{3.2}$$

where $\langle\cdot,\cdot\rangle$ represents the usual inner product in $L^2(I, K)$, and X, Y represent the solution space and test space, respectively. To explain the time discretization of variational type Problem(3.1).

Characterize the function $t \to \tilde{\mathbf{u}}(t)$, and we define the space $C(I,K) = C^0(I,K)$ as the space of continuous functions $\tilde{u} : I \to K$ equipped with the norm

$$\|\tilde{\mathbf{u}}\|_{C(I,K)} = \sup_{t\in I} \|\tilde{\mathbf{u}}\|_K.$$

We will use the space $L^2(I,K)$ as the space of discontinuous functions, which is given by

$$L^2(I,K) = \left\{\tilde{u} : I \to K : \|\tilde{\mathbf{u}}\|_{L^2(I,K)} = \left(\int_I \|\tilde{\mathbf{u}}\|_K^2 dt < \infty\right)^{1/2}\right\}.$$

In time discretization, we split the intervals I into N sub-intervals $I_n = [t_{n-1},\ t_n]$, where $n = 1, \cdots, N$ and $0 = t_0 < t_1 < t_2 < \cdots < t_{N-1} < t_N = T$. The symbol τ will indicate the time discretization parameter, as well as the maximum time step size $\tau = \max\limits_{1\le n\le N} \tau_n$, where $\tau_n = t_n - t_{n-1}$, the length of nth time interval I_n. The following set of time intervals $M_\tau = \{\bar{I}_1, \cdots, \bar{I}_N\}$ will be called the time-mesh. We find out the solution $\tilde{\mathbf{u}} : I \to K$ on each time interval I_n by a function $\tilde{\mathbf{u}}_\tau : I \to K$ which is a piecewise polynomial of some order l w.r.t time. The time-discrete solution space for $\tilde{\mathbf{u}}_\tau$ is $X_\tau^l \subset X$ and is defined by

$$X_\tau^l = \{\tilde{\mathbf{u}} \in C(I,K) : \tilde{\mathbf{u}}|_{I_n} \in \mathbb{P}_l(I_n,K) \text{ for all } I_n \in M_\tau\}, \tag{3.3}$$

where

$$\mathbb{P}_l(I_n,K) = \{\tilde{\mathbf{u}} : I_n \to K : \tilde{\mathbf{u}}(t) = \sum_{s=0}^{l} U^s t^s,\ for\ all\ t \in I_n,\ U^s \in K,\ \forall\ s\}.$$

The discrete test space for $\tilde{\mathbf{u}}_\tau$ is $Y_\tau^l \subset Y$ and is defined by

$$Y_\tau^k = \{v \in L^2(I,K) : v|_{I_n} \in \mathbb{P}_{k-1}(I_n,K) \quad \forall\ I_n \in M_\tau\}, \tag{3.4}$$

which is composed of $l-1$ piecewise polynomials and is discontinuous at the time step end nodes. We multiply Eq (3.1) by the test function $v_\tau \in Y_\tau^k$ and integrate it over the whole interval I. We get the discrete-time problem: Find $\tilde{\mathbf{u}}_\tau \in X_\tau^k$ such that $\tilde{\mathbf{u}}_\tau(0) = 0$ and

$$\int_I \langle \tilde{\mathbf{u}}_\tau'(t), v_\tau(t)\rangle\, dt = \int_I \langle F(t, \tilde{\mathbf{u}}_\tau(t), v_\tau(t))\rangle\, dt \ \ \forall\ v_\tau \in Y_\tau^l, \tag{3.5}$$

where $\langle\cdot,\cdot\rangle$ represents the usual inner product in $L^2(I,K)$. This discretization is known as the exact *continuous* Galerkin-Petrov method or briefly the "exact cGP(l)-method" of order k. The Galerkin-Petrov name is due to the fact that the solution space X_τ^l is different from the test space Y_τ^l. The term "exact" denotes that the time integral on the right-hand side of the Eq (3.5) is determined exactly. Because the discrete test space Y_τ^l is discontinuous, Eq (3.5) can be solved in a time marching procedure in which local problems on the time interval are handled successively. Therefore, we choose the test function $v_\tau(t) = v\psi(t)$ with arbitrary time-independent $v \in K$ and a scalar function $\psi : I \to \mathbb{R}$ which is zero on $I|_{I_n}$ and a polynomial of the order less than or equal to $l-1$ on the time interval $I_n = [t_{n-1},\ t_n]$. Then, we get from (3.5) the I_n-problem of the exact continuous Galerkin-Petrov method of order l: Find $\tilde{\mathbf{u}}_\tau|_{I_n} \in \mathbb{P}_l(I_n,K)$ such that

$$\int_{I_n} \langle d_t\tilde{\mathbf{u}}_\tau(t), v\rangle\psi(t)\, dt = \int_{I_n} \langle F(t, \tilde{\mathbf{u}}_\tau(t)), v\rangle\psi(t)\, dt \quad \forall\ v \in K\ \ \forall\psi \in \mathbb{P}_{l-1}(I_n), \tag{3.6}$$

with the initial condition $\tilde{\mathbf{u}}_\tau|_{I_n}(t_{n-1}) = \tilde{\mathbf{u}}_\tau|_{I_{n-1}}(t_{n-1})$ for $n \geq 2$ and $\tilde{\mathbf{u}}_\tau|_{I_n}(t_{n-1}) = \tilde{u}_0$ for $n = 1$.

In the usual case of a nonlinear function $F\langle\cdot,\cdot\rangle$, (where $\langle\cdot,\cdot\rangle$ denotes the usual inner product in L^2 norm) we need to calculate the integrals numerically on the right hand side of the Eq (3.6). The $(l+1)$-point Gauss-Lobatto formula is exact if the function is to be integrated as a polynomial of degree less than or equal to $2l-1$. As a result, this formula is applied to the integral on the left hand side of (3.6) will give the exact value. Then, the "I_n-problem of the numerically integrated cGP(l) method" is: Find $\tilde{\mathbf{u}}_\tau|_{I_n} \in \mathbb{P}_l(I_n, K)$ such that $\tilde{\mathbf{u}}_\tau(t_{n-1}) = \tilde{\mathbf{u}}_{n-1}$,

$$\sum_{s=0}^{l} \hat{w}_s d_t \tilde{\mathbf{u}}_\tau(t_{n,s})\psi(t_{n,s}) = \sum_{s=0}^{k} \hat{w}_s F(t_{n,s}, \tilde{\mathbf{u}}_\tau(t_{n,s}))\psi(t_{n,s}) \qquad \forall\ \psi \in \mathbb{P}_{l-1}(I_n), \tag{3.7}$$

where $\hat{w}_s$ are the weights and $\hat{t} \in [-1, 1], s = 0, 1, 2, 3, \ldots, l$ represent the nodes on the reference interval. To find $\tilde{\mathbf{u}}_\tau$ on each time interval I_n, we represent it by a polynomial ansatz

$$\tilde{\mathbf{u}}_\tau(t) = \sum_{s=0}^{k} U_n^s \phi_{n,s}(t) \quad \forall\ t \in I_n, \tag{3.8}$$

where the coefficients U_n^s are the components of K and the real-valued functions $\phi_{n,s} \in \mathbb{P}_l(I_n)$ are the Lagrange basis functions with respect to $l+1$ suitable nodal points $t_{n,s} \in I_n$ satisfying conditions mentioned below:

$$\phi_{n,s}(t_{n,r}) = \delta_{r,s}, \qquad r, s = 0, 1, 2, \ldots, l, \tag{3.9}$$

where $\delta_{r,s}$ is the Kronecker delta that is defined as:

$$\delta_{r,s} = \begin{cases} 1 & \text{if } r = s \\ 0 & \text{if } r \neq s \end{cases}$$

Like in [36], the $t_{n,s}$ have been defined as the quadrature points of $(l+1)$-point Gauss-Lobatto formula on the time interval I_n. For the selection of initial conditions we can set $t_{n,0} = t_{n-1}$ which implies the initial condition for (3.6)

$$\begin{aligned} U_n^0 &= \tilde{\mathbf{u}}_\tau|_{I_{n-1}} \ \text{ if } n \geq 2, \\ \text{for } n = 1 &\Rightarrow U_n^0 = \tilde{u}_0. \end{aligned} \tag{3.10}$$

We define the basis functions $\phi_{n,s} \in \mathbb{P}_l(I_n)$ via the affine reference transformation $\bar{T} : \hat{I} \to I_n$ where $\hat{I}$=[-1, 1] and

$$t = \bar{T}(\hat{t}) = \frac{t_n + t_{n-1}}{2} + \frac{\tau_n}{2}\hat{t} \in I_n \quad \forall\ \hat{t} \in I_n,\ n = 1, 2, 3 \ldots, N. \tag{3.11}$$

Let $\hat{\phi}_s \in \mathbb{P}_l(\hat{I})$, s=0, 1, …, l, demonstrate the basis functions that meet the requirements

$$\hat{\phi}_s(\hat{t}_r) = \delta_{r,s}, \qquad r, s = 0, 1, \ldots, l,$$

where $\hat{t}_0 = -1$ and $\hat{t}_r$, $r = 1, 2, \ldots, l$, are the quadrature points for the reference interval $\hat{I}$. Then, we define the basis functions on the original time interval I_n by the mapping

$$\phi_{n,s}(t) = \hat{\phi}_s(\hat{t}) \qquad \text{with} \qquad \hat{t} = \bar{T}_n^{-1}(t) = \frac{2}{\tau_n}(t + \frac{t_{n-1} - t_n}{2}) \in \hat{I}. \tag{3.12}$$

Likewise, the test basis functions $\psi_{n,r}$ are defined by the suitable reference basis functions $\hat{\psi} \in \mathbb{P}_{l-1}(\hat{I})$, i.e.,

$$\psi_{n,r}(t) = \hat{\psi}_r(\bar{T}_n^{-1}(t)) \quad \forall\ t \in I_n,\ r = 1, 2, \ldots, l.$$

From the representation (3.8), we get for $d_t\tilde{u}_\tau$

$$d_t\tilde{u}_\tau(t) = \sum_{s=0}^{k} U_n^s \phi'_{n,s}(t) \quad \forall\ t \in I_n. \tag{3.13}$$

By putting (3.13) in (3.6), we get

$$\int_{I_n} \langle d_t\tilde{\mathbf{u}}_\tau(t), v\rangle \psi(t)\, dt = \int_{I_n} \langle \sum_{s=0}^{l} U_n^s, v\rangle \phi'_s(t)\psi(t). \tag{3.14}$$

The integral is now transformed into the reference interval *hatI* and computed using the $(l+1)$-point Gauss-Lobatto quadrature formula, which leads for each test basis function $\psi \in \mathbb{P}_{l-1}$ and for all $v \in K$,

$$\begin{aligned} &\int_{\hat{I}_n} \sum_{s=0}^{l} \langle U_n^s, v\rangle \hat{\phi}'_s(\hat{t})\hat{\psi}(\hat{t})d\hat{t} = \int_{\hat{I}_n} \left\langle F\Big(\omega_n(\hat{t}), \sum_{s=0}^{l} U_n^s(\hat{t})\Big), v\right\rangle \hat{\psi}(\hat{t})d\hat{t} \quad \forall\ \ v \in K, \\ &\Rightarrow \sum_{\mu=0}^{l} \hat{w}_\mu \sum_{s=0}^{l} \langle U_n^s, v\rangle \hat{\phi}'_s(\hat{t}_\mu)\hat{\psi}(\hat{t}_\mu) = \sum_{\mu=0}^{l} \hat{w}_\mu \left\langle F\Big(\omega_n(\hat{t}_\mu), \sum_{s=0}^{l} U_n^s \hat{\phi}_s(\hat{t}_\mu)\Big), v\right\rangle \hat{\psi}(\hat{t}_\mu), \end{aligned} \tag{3.15}$$

where $\hat{w}_\mu$ are the weights and $\hat{t}_\mu \in [-1, 1]$ are the points of integration with $\hat{t}_0 = -1$ and $\hat{t}_l = 1$. If we choose the test functions $\psi_{n,i} \in \mathbb{P}_{l-1}(I_n)$ such that

$$\hat{\psi}(\hat{t_\mu}) = (\hat{w})^{-1}\delta_{r,\mu} \quad r, \mu = 1, 2, \ldots, l. \tag{3.16}$$

Now find the coefficients that are unknown $U_n^s \in K$ for $s = 1, \ldots, l$,

$$\sum_{s=0}^{l} \alpha_{r,s} U_n^s = \frac{\tau_n}{2}\{F(t_{n,r}, U_n^s) + \beta_r F(t_{n,0}, U_n^s)\} \quad \forall\ i = 1, 2, \ldots, l, \tag{3.17}$$

where $U_n^s = U_{n-1}^s$ for $n > 1$, $U_1^0 = \tilde{\mathbf{u}}_0$ for $n = 1$ and

$$\alpha_{r,s} = \hat{\phi}'_s(\hat{t_r}) + \beta_r\hat{\phi}'_s(t_0), \quad \beta_r = \hat{w}_0\hat{\psi}_r(\hat{t}_0).$$

We will discuss the cGP(k) method for the cases $l = 1$ *and* $l = 2$ in the following.

3.1.1. The cGP(1) method

We used the two point Gauss-Lobatto formula with $t_{n,0} = t_{n-1},\ t_{n,1} = t_n$ and weights $\hat{w}_0 = \hat{w}_1 = 1$, which gives the well-known Trapezoidal rule. We obtain $\alpha_{1,0} = -1, \alpha_{1,1} = 1$ and $\beta_1 = 1$. For the single coefficient $U_n^1 = \tilde{\mathbf{u}}_\tau(t_n) \in K$, the problem leads to the following block equation:

$$\alpha_{1,1}U_n^1 - \alpha_{n,0}U_n^0 \ = \ \frac{\tau_n}{2}\{F(t_n, U_n^1) + F(t_{n-1}, U_n^0)\}. \tag{3.18}$$

3.1.2. The cGP(2) method

The three-point Gauss-Lobatto formula (Simpson rule) is used to define the quadratic basis functions with weights $\hat{w}_0 = \hat{w}_2 = 1/3, \hat{w}_1 = 4/3$ and $\hat{t}_0 = -1, \hat{t}_1 = 0, \hat{t}_2 = 1$. Then, we get

$$\alpha_{r,s} = \begin{pmatrix} -\frac{5}{4} & 1 & \frac{1}{4} \\ 2 & -4 & 2 \end{pmatrix}, \quad \beta_r = \begin{pmatrix} \frac{1}{2} \\ -1 \end{pmatrix}, \quad r = 1, 2, \quad s = 0, 1, 2.$$

Thus, the system to be solved for $\mathbf{U}_n^1, \mathbf{U}_n^2 \in \mathbf{K}$ from the known $\mathbf{U}_n^0 = \mathbf{U}_{n-1}^2$ becomes:

$$\alpha_{1,1}\mathbf{U}_n^1 + \alpha_{1,2}\mathbf{U}_n^2 = -\alpha_{1,0}\mathbf{U}_n^0 + \frac{\tau_n}{2}\Big\{\mathbf{F}(t_{n,1}, \mathbf{U}_n^1) + \beta_1\mathbf{F}(t_{n,0}, \mathbf{U}_n^0)\Big\}, \tag{3.19}$$

$$\alpha_{2,1}\mathbf{U}_n^1 + \alpha_{2,2}\mathbf{U}_n^2 = -\alpha_{2,0}\mathbf{U}_n^0 + \frac{\tau_n}{2}\Big\{\mathbf{F}(t_{n,2}, \mathbf{U}_n^2) + \beta_2\mathbf{F}(t_{n,0}, \mathbf{U}_n^0)\Big\}, \tag{3.20}$$

where $\mathbf{U}_n^0$ indicate the initial conditions at the current time interval. For the cGP(k)-method, the discrete solution space consists of continuous piecewise polynomial functions in time of degree $k > 1$ and the discrete test space of discontinuous Galerkin (dG) having polynomial functions of degree $k-1$ (see [33–36] for more details). In the dG(k)-method, both the solution and test space are constructed by means of discontinuous polynomial functions of degree k. With respect to the computational costs, which mainly depend on the size of the resulting block system that has to be solved for each time interval, the cGP(k)-method is comparable to the dG($k-1$)-method. However, concerning the discretization error in time, the accuracy of the cGP(k)-method is one order higher than that of the dG($k-1$)-method. Furthermore, it is known that all cGP(k)-methods are A-stable, while all dG(k)-methods are even strongly A-stable (or L-stable), i.e., the dG-methods have better damping properties with respect to high frequency error components (see [33–36] for more details).

3.2. The Runge-Kutta method

This method is very well-known of order four established by Kutta [39] and extensively utilized for initial value problems (see [40] for more details). The Runge-Kutta method of order four is used to solve numerically the first order initial value problems. Let

$$\dot{y} = g(t, y), \quad a \le t \le b, \tag{3.21}$$

be the initial value problem with the initial condition $y(a) = \alpha$, and let $N > 0$ be an integer and set $h = \frac{b-a}{N}$ is the step size. Partition the whole interval into N sub-intervals with mesh points $t_i = a + ih$, for $i = 0, 1, 2, \cdots, N-1$. Then, the Runge-Kutta method of order four is described as

$$y_{i+1} = y_i + \frac{1}{6}(k_1 + 2(k_2 + k_3) + k_4), \ \text{ for } \ i = 0, 1, 2, \cdots, N-1, \tag{3.22}$$

where

$$\begin{aligned} k_1 &= hg(t_i, y_i), \\ k_2 &= hg(t_i + \frac{h}{2}, y_i + \frac{k_1}{2}), \\ k_3 &= hg(t_i + \frac{h}{2}, y_i + \frac{k_2}{2}), \\ k_4 &= hg(t_i + h, y_i + k_3). \end{aligned} \tag{3.23}$$

The Runge Kutta method of order four (RK-4) agrees with the Taylor series method up to terms of $O(h^4)$. This method can be extended to solve a system of n first-order differential equations. The generalization of the method is as follows.
Let

$$\begin{aligned}
\frac{dy_1}{dt} &= g_1(t, y_1, y_2, \ldots, y_n),\\
\frac{dy_2}{dt} &= g_2(t, y_1, y_2, \ldots, y_n),\\
&\vdots\\
\frac{dy_n}{dt} &= g_n(t, y_1, y_2, \ldots, y_n),
\end{aligned} \tag{3.24}$$

be the nth-order system of first-order initial value problems with the initial conditions

$$y_1(a) = \alpha_1,\ y_2(a) = \alpha_2, \cdots, y_n(a) = \alpha_n.$$

Use the notation y_i^j, for each $i = 0, 1, 2, \cdots, N$ and $j = 1, 2, \cdots, n$, to denote an approximation to $y^j(t_i)$. That is, y_i^j approximates the *jth* solution $y^(t)$ of (3.24) at the *ith* mesh points t_i. For the initial condition, set

$$y_0^1 = \alpha_1,\ y_0^2 = \alpha_2, \cdots, y_0^n = \alpha_n.$$

Suppose that the values $y_i^1,\ y_i^2, \cdots, y_i^n$ have been computed. We obtain $y_{i+1}^1,\ y_{i+1}^2, \cdots, y_{i+1}^n$ by first calculating

$$k_1^j = hg_j(t_i, y_i^1, y_i^2, \ldots, y_i^n), \tag{3.25}$$

$$k_2^j = hg_j(t_i + \frac{h}{2}, y_i^1 + \frac{k_1^1}{2}, y_i^2 + \frac{k_1^2}{2}, \ldots, y_i^n + \frac{k_1^n}{2}), \tag{3.26}$$

$$k_3^j = hg_j(t_i + \frac{h}{2}, y_i^1 + \frac{k_2^1}{2}, y_i^2 + \frac{k_2^2}{2}, \ldots, y_i^n + \frac{k_2^n}{2}), \tag{3.27}$$

$$k_4^j = hg_j(t_i + h, y_i^1 + k_3^1, y_i^2 + k_3^2, \ldots, y_i^n + k_3^n), \tag{3.28}$$

for each $j = 1, 2, \cdots, n$; and then

$$y_{i+1}^j = y_i^j + \frac{1}{6}(k_1^j + 2(k_2^j + k_3^j) + k_4^j), \tag{3.29}$$

for each $j = 1, 2, \cdots, n$. The values $k_1^1, k_1^2, \cdots, k_1^n$, must be computed before any of the terms of the form k_2^j can be determined.

3.3. Numerical simulations and discussions

This section relates to the implementation of the cGP(2)-scheme and RK4 scheme for the model presented and figure out the correct results. All the parameters, values are presented in Table 1. The findings and absolute errors achieved utilizing cGP(2) scheme (at $\tau = 0.1$) and RK4 method (at $\tau = 0.1$) were compared and presented in Tables 2–5 and in Figure 2. The findings achieved utilizing the presented approach are considerably comparable to those obtained using the RK4-method with

differing computational time. From comparison one could see that the results are not precise but similar up to nine digits approximately. The results demonstrated that the proposed methodologies yielded reliable and precise solutions and that both results overlapped significantly during the stipulated time period. We also solved the model using cGP(4) scheme (at $\tau = 0.2$) and RK4 (at $\tau = 0.1$) and found the absolute errors between the findings. Comparing the absolute values of the errors presented in Tables 6–9, we see that the higher order method cGP(4) achieves with a quite large time step size higher accuracy than the lower order method cGP(2) with smaller time step displayed in Tables 2–5. Moreover, the analysis of the numerical costs for different step sizes in terms of time show that the cGP(2)-method is more time consuming as in comparison to RK4-method as presented in Table 10 and Figure 2e. Furthermore, Figure 1 depicts the influence of varying the parameters ξ_1 and ψ_2 on the dynamical behavior of the state variables. By boosting the value of ξ_1, we observed that the population of susceptible individuals grows, and the population of infected individuals with acute HBV, infected individuals with chronic HBV and recovered individuals declines. By increasing ψ_2, the concentration of susceptible and recovered people increases, whereas the population of acutely infected and chronically infected individuals declines. Also, graphical visualizations of error solutions and errors phase portraits using cGP(2)-scheme (at $\tau = 0.0005$ where τ is the step size) and RK4-scheme (at $\tau = 0.0005$) are shown in Figure 3 for $t \in [0, 10]$. The findings demonstrate that the cGP(2) scheme outperforms the RK4 scheme in terms of time step accuracy while incurring higher computational costs.

Table 2. The comparative analysis of the outcomes of Galerkin and RK4 methods for $\tilde{S}$(t).

	$\lvert cGP(2)_{\tau=0.1} - RK4_{\tau=0.1}\rvert$		
t_i	cGP(2)-scheme	RK4-scheme	|cGP(2)-RK4|
0.0	100.000000000000	100.000000000000	0.00000000000000E-009
0.1	98.8923978777600	98.8923978779475	0.18746959540294E-009
0.2	97.8012267618895	97.8012267622551	0.36556002669386E-009
0.3	96.7261679090720	96.7261679096068	0.53472604122362E-009
0.4	95.6669105844358	95.6669105851311	0.69528027779597E-009
0.5	94.6231518165269	94.6231518173745	0.84763485119765E-009
0.6	93.5945961609257	93.5945961619179	0.99213082194183E-009
0.7	92.5809554721666	92.5809554732958	1.12910925054166E-009
0.8	91.5819486836314	91.5819486848903	1.25892540836503E-009
0.9	90.5973015951057	90.5973015964875	1.38184930165153E-009
1.0	89.6267466676998	89.6267466691980	1.49820778005960E-009

Table 3. The comparative analysis of the results of Galerkin and RK4 methods for $\tilde{I}_1(t)$.

	$\lvert cGP(2)_{\tau=0.1} - RK4_{\tau=0.1}\rvert$		
t_i	cGP(2)-scheme	RK4-scheme	|cGP(2)-RK4|
0.0	40.0000000000000	40.0000000000000	0.00000000000000E-009
0.1	40.6647754297249	40.6647754293823	0.34259528547409E-009
0.2	41.3115173101931	41.3115173095231	0.66994942926613E-009
0.3	41.9406193275814	41.9406193265987	0.98267349812886E-009
0.4	42.5524654340669	42.5524654327855	1.28134303167826E-009
0.5	43.1474301351317	43.1474301335651	1.56653356953029E-009
0.6	43.7258787669986	43.7258787651598	1.83877801873678E-009
0.7	44.2881677645815	44.2881677624830	2.09858086464010E-009
0.8	44.8346449203167	44.8346449179703	2.34645369801001E-009
0.9	45.3656496342260	45.3656496316431	2.58284416077004E-009
1.0	45.8815131555476	45.8815131527394	2.80822831655314E-009

Table 4. The comparative analysis of the results of Galerkin and RK4 methods for $\tilde{I}_2(t)$.

	$\lvert cGP(2)_{\tau=0.1} - RK4_{\tau=0.1}\rvert$		
t_i	cGP(2)-scheme	RK4-scheme	|cGP(2)-RK4|
0.0	20.0000000000000	20.0000000000000	0.0000000000000E-10
0.1	19.9106250505375	19.9106250505917	0.5414690917860E-10
0.2	19.8224827434847	19.8224827435910	1.0622258628246E-10
0.3	19.7355473148203	19.7355473149766	1.5628387473043E-10
0.4	19.6497935549745	19.6497935551789	2.0440538150979E-10
0.5	19.5651967956791	19.5651967959298	2.5065105546673E-10
0.6	19.4817328971831	19.4817328974781	2.9508484544749E-10
0.7	19.3993782358234	19.3993782361612	3.3777070029828E-10
0.8	19.3181096919390	19.3181096923178	3.7876546343796E-10
0.9	19.2379046381163	19.2379046385345	4.1812242557171E-10
1.0	19.1587409277559	19.1587409282118	4.5589843011840E-10

Table 5. The comparative analysis of the results of Galerkin and RK4 methods for $\tilde{R}(t)$.

	$\lvert cGP(2)_{\tau=0.1} - RK4_{\tau=0.1}\rvert$		
t_i	cGP(2)-scheme	RK4-scheme	|cGP(2)-RK4|
0.0	5.0000000000000	5.0000000000000	0.0000000000000E-10
0.1	5.5187126241351	5.5187126242367	1.0162182206841E-10
0.2	6.0378169434692	6.0378169436686	1.9942092421843E-10
0.3	6.5572635287196	6.5572635290131	2.9353230956985E-10
0.4	7.0770041268788	7.0770041272629	3.8408920488564E-10
0.5	7.5969916319757	7.5969916324469	4.7121240243087E-10
0.6	8.1171800566980	8.1171800572530	5.5502624718429E-10
0.7	8.6375245048468	8.6375245054825	6.3564797869731E-10
0.8	9.1579811445943	9.1579811453075	7.1318595473713E-10
0.9	9.6785071825168	9.6785071833045	7.8775030942779E-10
1.0	10.1990608383783	10.1990608392378	8.5944229510915E-10

Table 6. The comparative analysis of the outcomes of cGP(4) and RK4 methods for $\tilde{S}$(t).

	$\lvert cGP(4)_{\tau=0.2} - RK4_{\tau=0.1}\rvert$		
t_i	cGP(4)-scheme	RK4-scheme	|cGP(4)-RK4|
0.0	100.000000000000	100.000000000000	0.0000E-011
0.2	97.8012267622895	97.8012267622551	3.4404E-011
0.4	95.6669105851458	95.6669105851311	1.4694E-011
0.6	93.5945961618257	93.5945961619179	9.2200E-011
0.8	91.5819486848314	91.5819486848903	5.8904E-011
1.0	89.6267466691998	89.6267466691980	1.8048E-011

Table 7. The comparative analysis of the results of cGP(4) and RK4 methods for $\tilde{I}_1(t)$.

	$\lvert cGP(4)_{\tau=0.2} - RK4_{\tau=0.1}\rvert$		
t_i	cGP(4)-scheme	RK4-scheme	|cGP(4)-RK4|
0.0	40.0000000000000	40.0000000000000	0.0000E-011
0.2	41.3115173095931	41.3115173095231	7.0003E-011
0.4	42.5524654327669	42.5524654327855	1.8602E-011
0.6	43.7258787651986	43.7258787651598	3.8803E-011
0.8	44.8346449179167	44.8346449179703	5.3603E-011
1.0	45.8815131527576	45.8815131527394	1.8197E-011

Table 8. The comparative analysis of the results of cGP(4) and RK4 methods for $\tilde{I}_2(t)$.

	$\lvert cGP(4)_{\tau=0.2} - RK4_{\tau=0.1}\rvert$		
t_i	cGP(4)-scheme	RK4-scheme	|cGP(4)-RK4|
0.0	20.0000000000000	20.0000000000000	0.0000E-12
0.2	19.8224827435947	19.8224827435910	3.7019E-12
0.4	19.6497935551745	19.6497935551789	4.3983E-12
0.6	19.4817328974731	19.4817328974781	4.9987E-12
0.8	19.3181096923190	19.3181096923178	1.1973E-12
1.0	19.1587409282159	19.1587409282118	4.0998E-12

Table 9. The comparative analysis of the results of cGP(4) and RK4 methods for $\tilde{R}(t)$.

	$\lvert cGP(4)_{\tau=0.2} - RK4_{\tau=0.1}\rvert$		
t_i	cGP(4)-scheme	RK4-scheme	|cGP(4)-RK4|
0.0	5.0000000000000	5.0000000000000	0.0000E-13
0.2	6.0378169436682	6.0378169436686	3.9968E-13
0.4	7.0770041272628	7.0770041272629	1.0036E-13
0.6	8.1171800572580	8.1171800572530	5.0004E-13
0.8	9.1579811453043	9.1579811453075	3.2010E-13
1.0	10.199060839238	10.199060839237	4.9916E-13

Table 10. The computational costs in terms of the CPU time (in seconds) for the Galerkin-scheme and RK4 scheme $t \in [0,1]$.

CPU time (in seconds)		
$1/\tau$	Galerkin-scheme	RK4-scheme
10	0.254317	0.054033
100	0.377437	0.042027
200	0.732050	0.065334
500	1.393989	0.117353
1000	2.039698	0.144833
1500	2.835332	0.151022
5000	5.925991	0.173021
10000	10.267904	0.243410
20000	20.300213	0.466144
100000	283.102165	5.214400

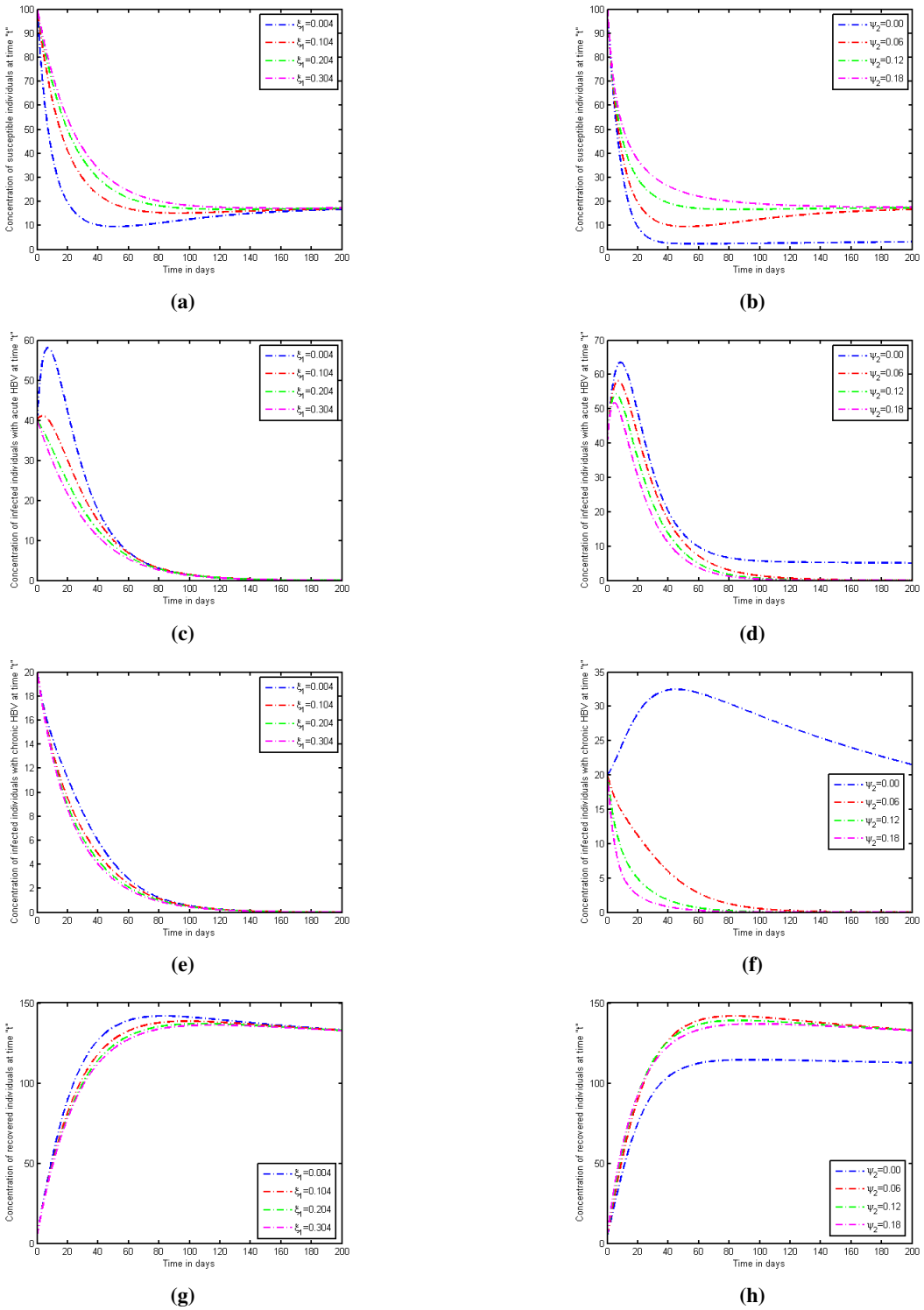

Figure 1. The influence of changing ξ (left) and ψ (right) on the dynamics of $\tilde{S}(t)$, $\tilde{I}_1(t)$, $\tilde{I}_2(t)$ and $\tilde{R}(t)$ for t∈[0, 200].

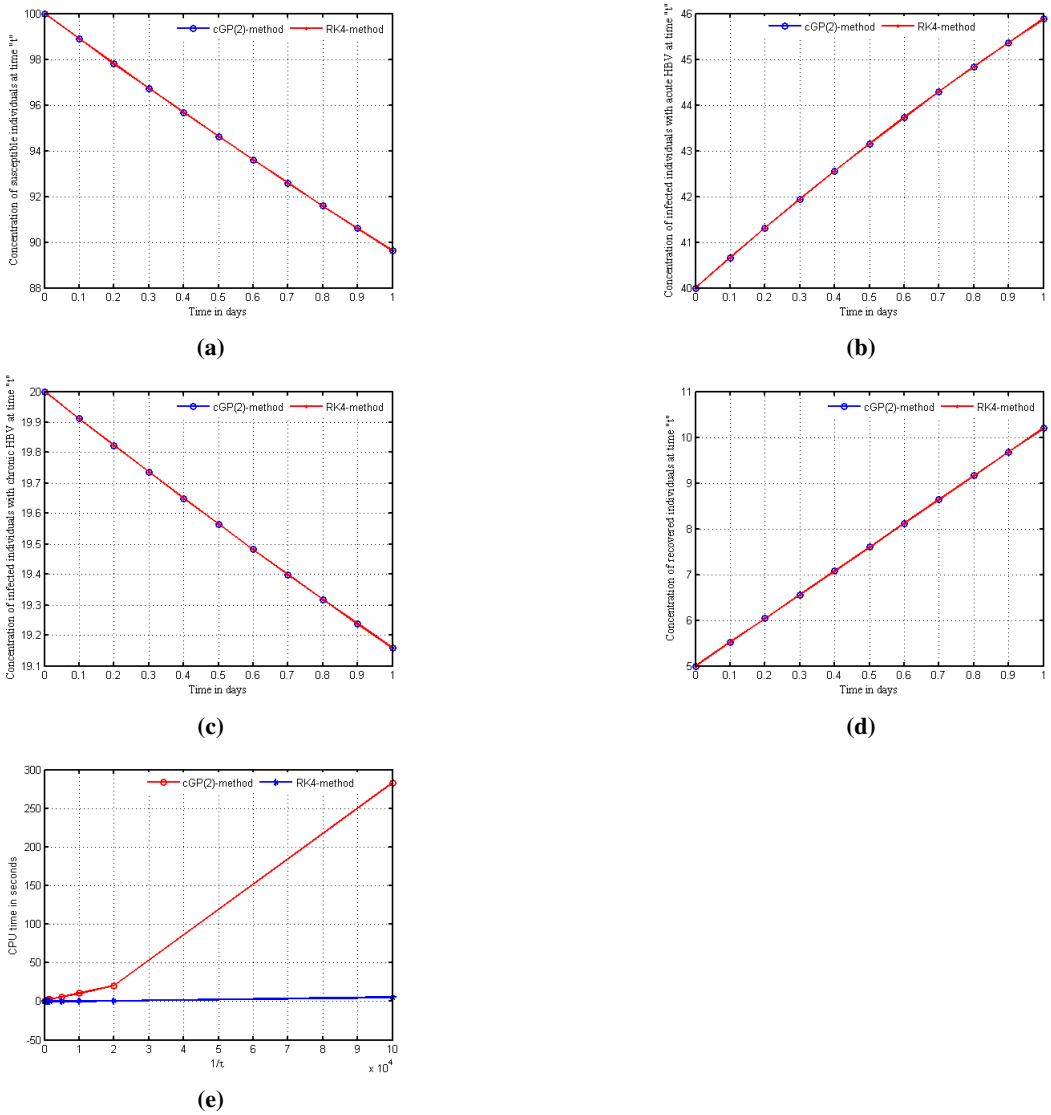

Figure 2. Graphical comparison using Galerkin-scheme ($\tau = 0.1$) and RK4-scheme ($\tau = 0.1$) for $\tilde{S}(t)$, $\tilde{I}_1(t)$, $\tilde{I}_2(t)$ and $\tilde{R}(t)$ for t∈[0, 1] and computational costs in terms of time for both schemes.

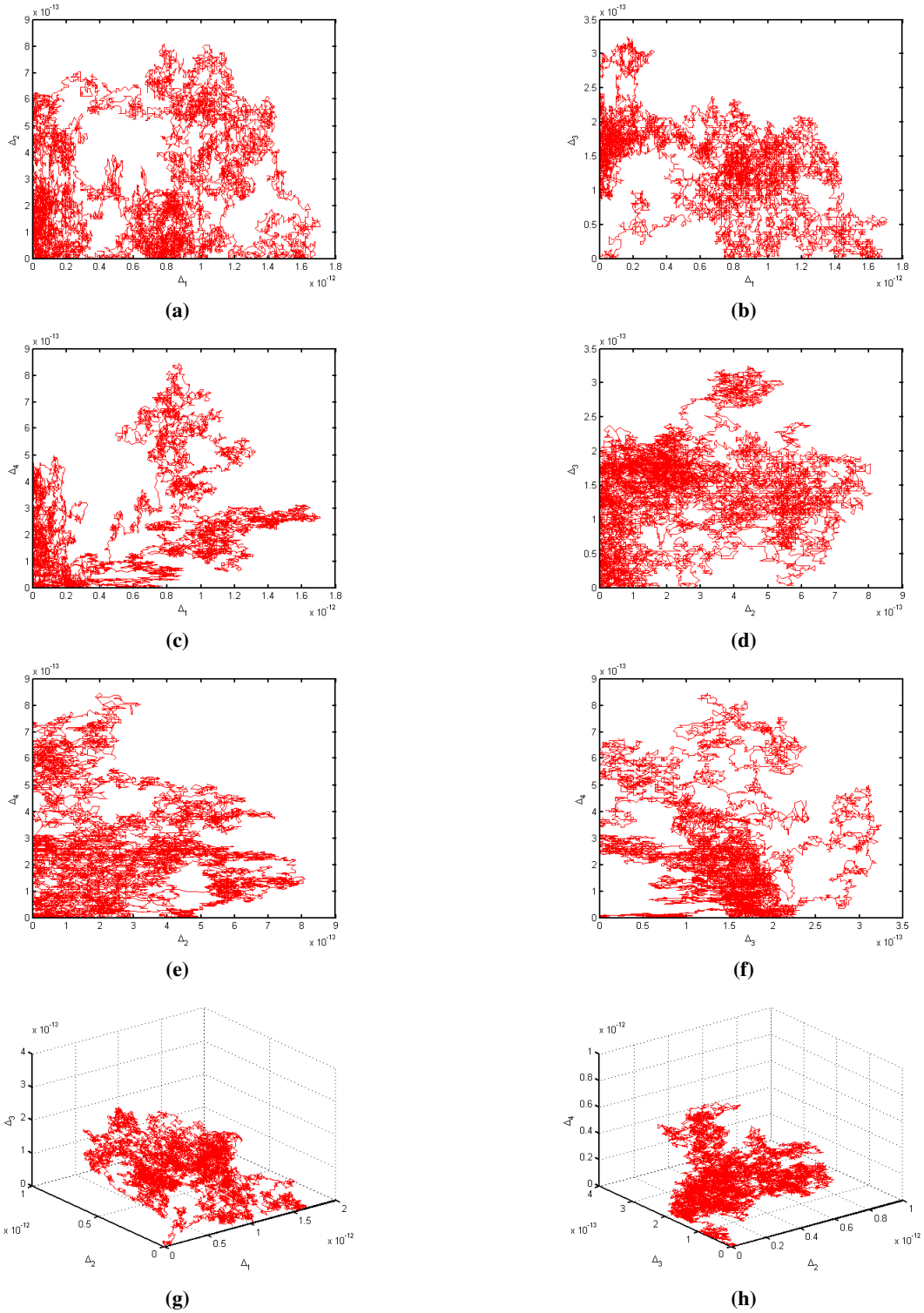

Figure 3. The geometrical representation of errors solutions and error phase portraits using Galerkin-scheme ($\tau = 0.0005$) and RK4-scheme ($\tau = 0.0005$) for $t \in [0,10]$.

3.4. The Basic information of the computer used for simulations

- Windows: 8.1 single language
- Processor: Intel(R)Core(TM)i5-5200CPU@2.20GHz 2.20GHz
- Installed memory(RAM): 4.00GB
- System type: 64 bit Operating System, x64-based processor

4. Example 1: The Chen system

The Chen system was initially established in 1999 by Chen and Ueta [41] and described as follows:

$$\frac{dX(t)}{dt} = \alpha(Y(t) - X(t)) \tag{4.1}$$

$$\frac{dY(t)}{dt} = (\gamma - \alpha)X(t) - X(t)Y(t) + \gamma Y(t) \tag{4.2}$$

$$\frac{dZ(t)}{dt} = X(t)Y(t) - \beta Z(t), \tag{4.3}$$

where $X(t)$, $Y(t)$ and $Z(t)$ are the dependent variables, and α, β and γ are positive constant parameters. According to bifurcation analysis assuming the parameters $\alpha = 35$ and $\gamma = 28$, system of Equations 4.1–4.3 shows non-chaotic and chaotic behaviour for $\beta = 12$ and $\beta = 3$, respectively [20].

For the Chen system solutions, Hussain et al. [20] employed and investigated the Galerkin-method for the model of both non-chaotic behavior and chaotic behavior. They numerically compared the Galerkin-method solutions to the classic RK4-method solutions and determined that the Galerkin solutions with larger time steps achieved comparable accuracy to the RK4 solutions with significantly smaller time steps. This opposed the claim that the findings of the Galerkin-method and RK4-method are same.

4.1. Chen system with non chaotic behavior

Herein, we consider the Chen system with non-chaotic behavior and implement the proposed methods for same and different step sizes to strengthen and confirm the claim that (1) the results of Galerkin and RK4 are not equal, as could be seen from Tables 11–16. The computations are conducted with several time step sizes, and the accuracy is assessed at various time intervals. It could be observed that the results are not similar at $\tau = 0.01$ while identical up to eight digit, when $\tau = 0.0001$. (2) Tables 17 and Figure 4(g) show the elapsed time of both schemes, and it may be worthy to note that the RK4-scheme required less time as compared to the cGP(2)-scheme. In addition, Figure 4 shows the differences between the outcomes obtained through the Galerkin and RK4 methods for different values of τ in the non-chaotic case. This confirms that the $RK4$ technique requires less computing cost than the Galerkin scheme.

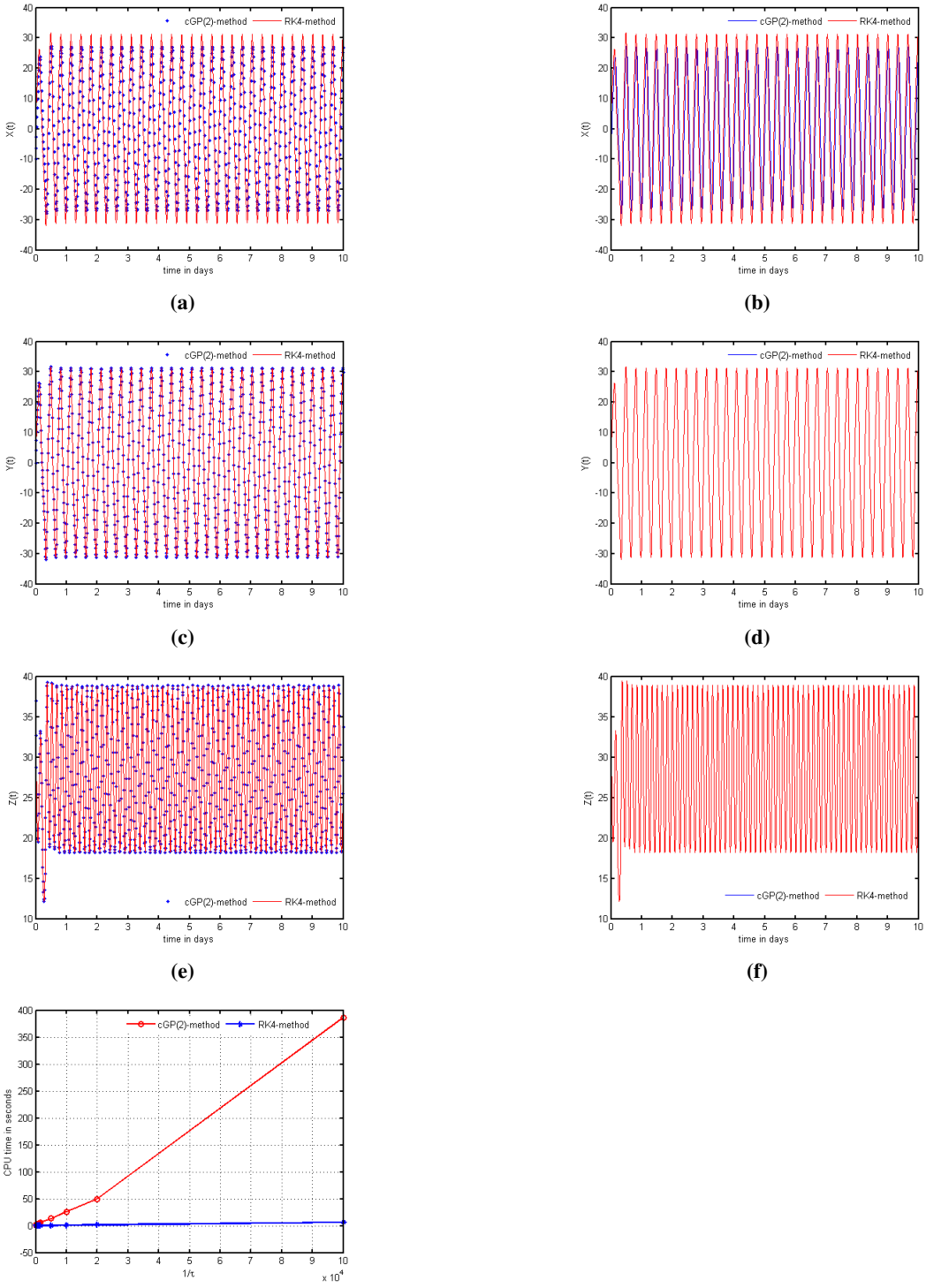

Figure 4. Comparison of Galerkin-scheme ($\tau = 0.01$) and $RK4$-scheme ($\tau = 0.01$) (Left) versus Galerkin-scheme ($\tau = 0.0001$) and $RK4$-scheme ($\tau = 0.0001$) (Right) for $X(t)$, $Y(t)$ and $Z(t)$ where $t \in [0, 10]$ along with computational cost in terms of time.

Table 11. Differences in Galerkin and RK4 outcomes for $X(t)$.

	$\lvert\text{Galerkin}_{\tau=0.01} - \text{RK4}_{\tau=0.01}\rvert$		
t_i	Galerkin-scheme	RK4-scheme	|Galerkin-RK4|
1	-27.048832665674844	-27.054660707952376	0.005828042277532
2	-24.121382804250171	-24.220203102041907	0.098820297791736
3	-17.595913326656611	-17.836012791172081	0.240099464515470
4	-9.479112397807544	-9.831210400585679	0.352098002778135
5	-1.519967659034344	-1.930913832633865	0.410946173599521
6	5.629377958266195	5.185500567394190	0.443877390872006
7	12.096029332377837	11.616145579345067	0.479883753032770
8	18.108332396521128	17.598089053219176	0.510243343301951
9	23.372140795726757	22.908872091375947	0.463268704350810
10	26.704118501387580	26.483143514708306	0.220974986679273

Table 12. Differences in Galerkin and RK4 solutions for $Y(t)$.

	$\lvert\text{Galerkin}_{\tau=0.01} - \text{RK4}_{\tau=0.01}\rvert$		
t_i	Galerkin-scheme	RK4-scheme	|Galerkin-RK4|
1	-25.757727035512879	-25.829785688541214	0.072058653028336
2	-15.733229367223030	-15.960756261129955	0.227526893906925
3	-4.687271172508644	-5.014096669129265	0.326825496620621
4	4.359806983134549	4.021272883035516	0.338534100099033
5	11.202102936238061	10.866833989119010	0.335268947119051
6	16.973500381147989	16.603394521003853	0.370105860144136
7	22.551140692377597	22.122303983970319	0.428836708407278
8	27.775451248198650	27.358265955699231	0.417185292499418
9	31.042892281454858	30.879307980173685	0.163584301281173
10	29.717909515486923	30.160333148606682	0.442423633119759

Table 13. Differences in cGP(2) and $RK4$ solutions for $Z(t)$.

	$\lvert\text{Galerkin}_{\tau=0.01} - RK4_{\tau=0.01}\rvert$		
t_i	Galerkin-scheme	$RK4$-scheme	|Galerkin-$RK4$|
1	37.235989947410992	37.195681864725273	0.040308082685719
2	38.702841501348885	38.727949536128541	0.025108034779656
3	34.855832136470781	35.030555096436252	0.174722959965472
4	28.471059015282727	28.746019629584858	0.274960614302131
5	22.625844253119464	22.890177162419192	0.264332909299728
6	18.991435889835248	19.140513211975794	0.149077322140545
7	18.286069422857828	18.221904191712490	0.064165231145338
8	20.890272803905422	20.521203756415815	0.369069047489607
9	26.631030747685497	25.950053980017987	0.680976767667509
10	33.728856634945707	32.981125844075343	0.747730790870364

Table 14. Differences in cGP(2) and $RK4$ solutions for $X(t)$.

	$\lvert\text{Galerkin}_{\tau=0.0001} - RK4_{\tau=0.0001}\rvert$		
t_i	Galerkin-scheme	$RK4$-scheme	$\lvert$Galerkin-$RK4\rvert$
1	-27.047610303301788	-27.047610303357622	0.005583444817603E-008
2	-24.094604479340664	-24.094604480173757	0.083309359411032E-008
3	-17.530298570737838	-17.530298572724817	0.198697946984794E-008
4	-9.383231382528516	-9.383231385407889	0.287937318432796E-008
5	-1.408518132110425	-1.408518135446550	0.333612537595229E-008
6	5.749603796814950	5.749603793216482	0.359846730191293E-008
7	12.226070443083062	12.226070439194331	0.388873111489829E-008
8	18.246170817362785	18.246170813251055	0.411172962344608E-008
9	23.495090238172907	23.495090234528103	0.364480357006869E-008
10	26.756926094741043	26.756926093227204	0.151383972024632E-008

Table 15. Differences in Galerkin and $RK4$ outcomes for $Y(t)$.

	$\lvert\text{Galerkin}_{\tau=0.0001} - RK4_{\tau=0.0001}\rvert$		
t_i	Galerkin-scheme	$RK4$-scheme	$\lvert$Galerkin-$RK4\rvert$
1	-25.739166712238003	-25.739166712853841	0.061583804722432E-008
2	-15.671765498592148	-15.671765500480387	0.188823889857304E-008
3	-4.598724349917238	-4.598724352588283	0.267104471873836E-008
4	4.451217413219246	4.451217410479821	0.273942468709265E-008
5	11.292738780804578	11.292738778094927	0.270965117010746E-008
6	17.074033073890451	17.074033070883853	0.300659763752265E-008
7	22.667547308391388	22.667547304916646	0.347474227169187E-008
8	27.886618576432806	27.886618573137842	0.329496430140352E-008
9	31.079875020723971	31.079875019688370	0.103560182651563E-008
10	29.584671502608845	29.584671506692231	0.408338607371661E-008

Table 16. Differences in Galerkin and $RK4$ outcomes for $Z(t)$.

	$\lvert\text{Galerkin}_{\tau=0.0001} - RK4_{\tau=0.0001}\rvert$		
t_i	Galerkin-scheme	$RK4$-scheme	$\lvert$Galerkin-$RK4\rvert$
1	37.246938185955891	37.246938185624877	0.033101343888120E-008
2	38.695920712480053	38.695920712709558	0.022950530365051E-008
3	34.807827360519170	34.807827361976500	0.145733025647132E-008
4	28.396215621242757	28.396215623489454	0.224669705062297E-008
5	22.554831144255033	22.554831146374244	0.211921147297289E-008
6	18.952840363341220	18.952840364482952	0.114173204224244E-008
7	18.306723791470940	18.306723790831505	0.063943517147891E-008
8	20.994876585309012	20.994876582156568	0.315244363946476E-008
9	26.818990233189414	26.818990227565898	0.562351587518606E-008
10	33.927750982739248	33.927750976850653	0.588859450090240E-008

Table 17. The computational costs in terms of the CPU-time (in seconds) for the Galerkin and $RK4$ schemes for $t \in [0,10]$.

CPU time (in seconds)		
$1/\tau$	Galerkin-scheme	$RK4$-scheme
10	0.351107	0.049666
100	1.395488	0.060902
200	1.805245	0.064809
500	2.922045	0.098383
1000	4.807289	0.133293
1500	6.021356	0.169597
5000	13.376732	0.411494
10000	26.135305	1.037192
20000	49.576749	1.942809
100000	386.666995	6.432528

5. Example 2: HIV infection model description

In the field of HIV infection of healthy T-cells, mathematical models have become indispensable tools for better understanding the dynamical behaviour, transmission, disease progression, and immunological interactions of HIV. In humans, the HIV virus mainly targets healthy T-cells. Whenever HIV enters the body, it infects a significant number of healthy T-cells, causing their depletion gradually. As a consequence, the body's immune system is destroyed, weakening the host immunological response to viral diseases and eventually leading to acquired immunodeficiency syndrome (AIDS). The reduction in the number of these cells is used as a major indication to monitor the development of HIV infection and the symptoms of AIDS. These cells proliferate at a steady rate from bone marrow and thymus precursors. To characterize the dynamical behavior of HIV infection, several mathematical models have been introduced. The model proposed by Attaullah et al. [19] is as follows:

$$\frac{d\tilde{T}(t)}{dt} = s_0 - \mu_{\tilde{T}}\tilde{T}(t) + \alpha\tilde{T}(t)\left(1 - \frac{\tilde{T}(t) + \tilde{I}(t)}{\tilde{T}_{\max}}\right) - \beta\tilde{V}(t)\tilde{T}(t), \tag{5.1}$$

$$\frac{d\tilde{I}(t)}{dt} = \beta\tilde{V}(t)\tilde{T}(t) - \tilde{I}(t)\mu_{\tilde{I}}, \tag{5.2}$$

$$\frac{d\tilde{V}(t)}{dt} = \gamma\mu_{\tilde{I}}\tilde{I}(t) - \mu_{\tilde{V}}\tilde{V}(t). \tag{5.3}$$

Herein, $\tilde{T}$, $\tilde{I}$ and $\tilde{V}$ describe the densities of healthy/infected T-cells and virus respectively. The explanation of parameters, along their values and initial condition for the state variables are illustrated in Table 18.

The aforementioned model is considered as a model problem, and we implement the suggested methods. Table 19 and Figure 5 show the numerical cost in terms of time, and for all other results the readers are advised to see [19] for details. It is worth noting that the $RK4$ approach required very less time than the cGP(2) approach (see Table 19 and Figure 5). This is further supported by the fact that $RK4$ takes less time than cGP(2).

Table 18. The description of variables and parameters with their values (unit=day^{-1}mm^{-3}) [19].

Variable	Explanation	Value
$\tilde{T}(0)$	Density of healthy T-cells	0.1
$\tilde{I}(0)$	Density of infected T-cells	0
$\tilde{V}(0)$	Density of free HIV viruses	0.1
Parameters and constants		
s_0	The generation rate of healthy T-cells	0.1
α	Proliferating of healthy T-cells	3
$\mu_{\tilde{T}}$	Death rate healthy T-cells	0.02
$\mu_{\tilde{I}}$	Death rate infected T-cells	0.3
$\mu_{\tilde{V}}$	Death rate of free virus	2.4
β	The infection rate	0.0027
$\tilde{T}_{\max}$	Maximum number of healthy T-cells	1500
γ	Production rate of virus by infected T-cells	10

Table 19. In terms of CPU time (in seconds), the computational costs for Galerkin and $RK4$ schemes $t \in [0, 10]$.

CPU time (in seconds)		
$1/\tau$	cGP(2)-Method	$RK4$-Method
10	0.324928	0.061477
100	0.537519	0.062665
200	0.795505	0.073890
500	1.355163	0.105935
1000	2.381097	0.140199
1500	2.967904	0.154493
5000	6.112178	0.425491
10000	10.263549	0.852300
20000	19.683633	1.675098
100000	231.860883	6.786395

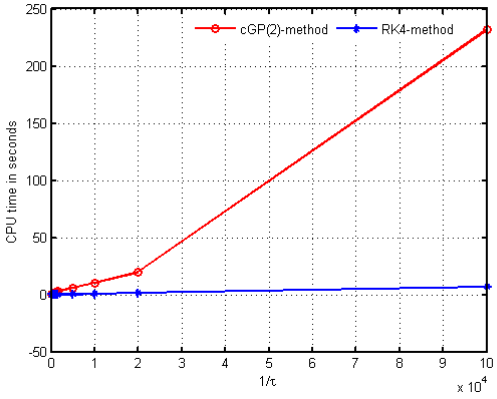

Figure 5. Graphical comparison for time elapsed by cGP(2)-scheme and $RK4$-scheme for different time step sizes.

6. Example 3: Model problem

In order to demonstrate that the provided temporal discretization technique is accurate and efficient in terms of time, as a test problem with the prescribed exact solution, analyze the implementations of the cGP(2) and $RK4$ approaches. The detail of the considered problem is given on page 332 of [42]. The problem consists of two differential equation as follows:

$$\frac{dU(t)}{dt} = -4U + 3V + 6, \tag{6.1}$$

$$\frac{dV(t)}{dt} = -2.4U + 1.6V + 3.6, \tag{6.2}$$

where the initial values are $U(0) = 0$ and $V(0) = 0$. The exact solution to the aforementioned model is

$$U(t) = -3.375\exp(-2t) + 1.875\exp(-0.4t) + 1.5, \tag{6.3}$$

$$V(t) = -2.25\exp(-2t) + 2.25\exp(-0.4t). \tag{6.4}$$

Performed different numerical tests to assess the accuracy of the suggested techniques utilized an equidistant and unequal time step size $\tau = T/N$ for all tests, with $T = 0.5$. First, find out the solutions using the cGP(2) and $RK4$ at $\tau = 0.1$ and then using at $\tau = 0.00125$ and $\tau = 0.000625$, respectively. To determine the numerical solution's accuracy, the numerical solutions were compared with the prescribed analytical exact solution presented in Tables 20 and 21. The computational results clearly demonstrate that the Galerkin-scheme gives highly accurate results at relatively large time step sizes as compared to RK4-scheme. For the same step size ($\tau = 0.1$), the Galerkin-scheme gained the accuracy of 10^{-5} while the $RK4$-method achieved the accuracy of 10^{-4}. Further, $RK4$ achieved the accuracy of 10^{-5} at $\tau = 0.000625$, while the Galerkin-method can already reach the same precision and accuracy with $\tau = 0.00125$. This is a clear negation to the claim of [28] that Galerkin and $RK4$ have the same results. On the other hand, we find the order of convergence and compared the experimental orders of convergence with the theoretical order of convergence. The cGP(2)-method is of order 3 in the whole time interval and super-convergent of order 4 at the discrete time points. One can see from Table 24 that the experimental orders of convergence for the cGP(2) method are much

more visible. From Table 24, we observe that the EOC coincides with the theoretical orders of convergence for corresponding time discretization schemes.

Moreover, we computed the required CPU-time in seconds at different time step sizes for the mentioned above system, as given in Table 25 and plotted in Figure 6 for both methods. It can be seen from Table 25 and Figure 6 that the $RK4$-scheme is much faster than the Galerkin-scheme. Hence, these numerical tests show that the Galerkin approach is less efficient and takes more time as in comparison to the $RK4$-method.

Table 20. Differences between the solutions of cGP(2)-scheme and exact solution for $U(t)$ and $V(t)$.

	cGP(2)-method	cGP(2)-method	Errors	Errors
t_i	$U_{(\tau=0.1)}$	$V_{(\tau=0.1)}$	$\lvert U_{\text{cGP(2)}} - U_{exact}\rvert$	$\lvert V_{\text{cGP(2)}} - V_{exact}\rvert$
0.0	0.000000000000000	0.000000000000000	0.000000000000000E-005	0.000000000000000E-005
0.1	0.538262676008231	0.319631223294469	0.123076418656609E-005	0.082037279897085E-005
0.2	0.968510978848033	0.568790332547925	0.201525662668622 E-005	0.134324181744194E-005
0.3	1.310734072202835	0.760743151897503	0.247482449533543E-005	0.164950454151214E-005
0.4	1.581281648929932	0.906331555404320	0.270148609193832E-005	0.180050590703473E-005
0.5	1.793524283491225	1.014413609321062	0.276457637293781E-005	0.184246865142512E-005

Table 21. Differences between the solutions of $RK4$-scheme and exact solution for $U(t)$ and $V(t)$.

	$RK4$-method	$RK4$-method	Errors	Errors
t_i	$U_{(\tau=0.1)}$	$V_{(\tau=0.1)}$	$\lvert U_{RK4} - U_{exact}\rvert$	$\lvert V_{RK4} - V_{exact}\rvert$
0.0	0.0000000	0.0000000	0.00000E-004	0.00000E-004
0.1	0.5382550	0.3196263	0.08285E-004	0.05803E-004
0.2	0.9684983	0.5687817	0.15140E-004	0.09596E-004
0.3	1.3107170	0.7607328	0.19070E-004	0.12160E-004
0.4	1.5812630	0.9063208	0.20980E-004	0.13110E-004
0.5	1.7935050	1.0144020	0.21930E-004	0.12400E-004

Table 22. Differences between the solutions of Galerkin-scheme and exact solution for $U(t)$ and $V(t)$.

	Galerkin-scheme	Galerkin-scheme	Errors	Errors
t_i	$U_{(\tau=0.00125)}$	$V_{(\tau=0.00125)}$	$\lvert U_{Galerkin} - U_{exact}\rvert$	$\lvert V_{\text{Galerkin}} - V_{exact}\rvert$
0.0	0.000000000000000	0.000000000000000	0.000000000000000E-013	0.000000000000000E-013
0.1	0.538263906772387	0.319632043667248	0.303090885722668E-013	0.218631863105119E-013
0.2	0.968512994104611	0.568791675789710	0.487387907810444E-013	0.399721318314869E-013
0.3	1.310736547027270	0.760744801402005	0.608402217494586E-013	0.549991745625225E-013
0.4	1.581284350415960	0.906333355910185	0.630606677987089E-013	0.674950994505733E-013
0.5	1.793527048067532	1.014415451789671	0.659472476627343E-013	0.779111596277818E-013

Table 23. Differences between the solutions of $RK4$-scheme and exact solution for $U(t)$ and $V(t)$.

	$RK4$-method	$RK4$-method	Errors	Errors
t_i	$U_{(\tau=0.000625)}$	$V_{(\tau=0.000625)}$	$\lvert U_{RK4} - U_{exact}\rvert$	$\lvert V_{RK4} - V_{exact}\rvert$
0.0	0.000000000000000	0.000000000000000	0.000000000000000E-013	0.000000000000000E-013
0.1	0.538263906772406	0.319632043667260	0.113242748511766E-013	0.319632043667268E-013
0.2	0.968512994104641	0.568791675789730	0.185407245112401E-013	0.568791675789742E-013
0.3	1.310736547027307	0.760744801402030	0.233146835171283E-013	0.760744801402045E-013
0.4	1.581284350415998	0.906333355910211	0.255351295663786E-013	0.906333355910227E-013
0.5	1.793527048067573	1.014415451789698	0.255351295663786E-013	1.014415451789714E-013

Table 24. Comparative analysis of orders of convergence for U and V.

cGP(2)-Scheme				
$\frac{1}{\tau}$	$\lVert U - U_\tau\rVert$	EOC	$\lVert V - V_\tau\rVert$	EOC
20	1.38E-04	2.29	1.35E-03	0.84
40	1.03E-05	3.75	8.86E-05	3.93
80	6.88E-07	3.90	5.60E-06	3.98
160	4.39E-08	3.97	3.51E-07	4.00
320	2.75E-09	4.00	2.19E-08	4.00
640	1.71E-10	4.01	1.37E-09	4.01

Table 25. The computational costs in terms of CPU time (in seconds) for the Galerkin-scheme and $RK4$ scheme t $\in$ [0,0.5].

CPU time (in seconds)		
$1/\tau$	Galerkin	$RK4$-Method
10	0.277157	0.044306
100	0.479595	0.045998
200	0.577860	0.051233
500	0.925523	0.076149
1000	1.758500	0.090703
1500	2.478847	0.150593
5000	5.433901	0.341417
10000	8.990064	0.569608
20000	14.029849	1.242083
100000	144.766793	5.873934

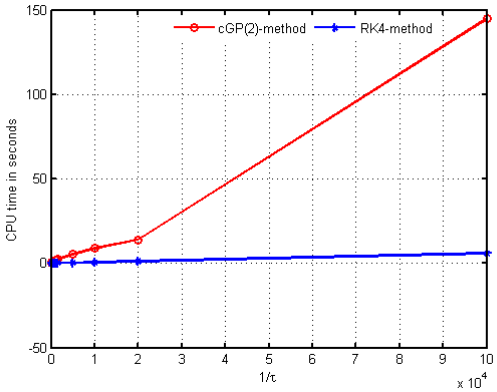

Figure 6. Graphical comparison for the time elapsed by Galerkin-scheme and $RK4$-scheme for different time step sizes.

7. Conclusions and future recommendations

In this work, a higher-order Galerkin and a fourth order classical Runge Kutta scheme were implemented. Various numerical tests were performed to determine the reliability and effectiveness of the described schemes. In addition, the impacts of increasing the parameters ξ_1 and ψ_2 on the dynamical behavior of the state variables were appropriately discussed. We noticed that increasing the value of ξ_1 increases the population of susceptible individuals while decreasing the population of infected individuals with acute HBV, infected individuals with chronic HBV and recovered individuals. By elevating ψ_2, the concentration of susceptible and recovered individuals grows, while the number of acutely and chronically infected people decreases. We executed many computational tests and compared the results quantitatively. According to computational simulations, the Galerkin-scheme provides much more accurate solutions at relatively high time step sizes than the $RK4$-method. Afterwards, the accuracy of the cGP(2) technique confirm that it produces more accurate results at relatively longer step sizes than the RK-4 scheme at a comparable numerical cost. The results of numerical studies revealed that the explicit $RK4$-scheme used less CPU time in comparison to the accuracy, but the implicit Galerkin-scheme required more CPU time. We proved that cGP(2) works better on time steps than the RK4 method. The proposed scheme could be applicable for solving complex real-world problems.

In the future, we plan to investigate the numerical and qualitative aspects of the present concept using different fractional order derivatives. The concept of fractional analysis is well known, and it has recently become a prominent study area. The utility of fractional calculus in modeling a wide range of real-world phenomena has been demonstrated. Using fractional order derivatives and integrals, researchers have researched infectious illnesses such as HIV, AIDS, and others.

Acknowledgments

This research received funding support from the NSRF via the Program Management Unit for Human Resources & Institutional Development, Research and Innovation, (grant number B05F650018).

Conflict of interest

The authors declare that they have no conflicts of interest.

References

1. C. Seeger, W. S. Mason, Hepatitis b virus biology, *Microbiol. Mol. Biol. R.*, **1** (2000), 51–68. https://doi.org/10.1128/MMBR.64.1.51-68.2000
2. B. Hepatitis, http://www. who. int/mediacentre/factsheets/fs204/en/index. html.
3. D. Candotti, O. Opare-Sem, H. Rezvan, F. Sarkodie, J. P. Allain, Molecular and serological characterization of hepatitis b virus in deferred ghanaian blood donors with and without elevated alanine aminotransferase, *J. Viral Hepatitis*, **13** (2006), 715–724. https://doi.org/10.1111/j.1365-2893.2006.00741.x
4. M. Kane, Global programme for control of hepatitis b infection, *Vaccine,* **13** (1995), S47–S49. https://doi.org/10.1016/0264-410x(95)80050-n
5. G. F. Medley, N. A. Lindop, W. J. Edmunds, D. J. Nokes, Hepatitis-b virus endemicity: Heterogeneity, catastrophic dynamics and control, *Nature medicine*, **7** (2001), 619–624. https://doi.org/10.1038/87953
6. J. Hou, Z. Liu, F. Gu, Epidemiology and prevention of hepatitis b virus infection, *Int. J. Med. Sci.*, **2** (2005), 50. https://doi.org/10.7150/ijms.2.50
7. Z. Wang, J. Zhang, H. Yang, X. Li, S. Wen, Y. Guo, et al., Quantitative analysis of hbv dna level and hbeag titer in hepatitis b surface antigen positive mothers and their babies: Hbeag passage through the placenta and the rate of decay in babies, *J. Med. Virol.*, **71** (2003), 360–366. https://doi.org/10.1002/jmv.10493
8. D. Z. Xu, Y. P. Yan, B. C. Choi, J. Q. Xu, K. Men, J. X. Zhang, et al., Risk factors and mechanism of transplacental transmission of hepatitis b virus: A case-control study, *J. Med. virol.*, **67** (2002), 20–26. https://doi.org/10.1002/jmv.2187
9. L. Robinson, COVID-19 and uncertainties in the value per statistical life, *Regulatory Rev.*, **8** (2020). https://doi.org/10.1001/jama.2020.19759
10. M. D. Cutler, H. L. Summers, The COVID-19 Pandemic and the 16 Trillion Virus, *JAMA*, **324** (2020), 1495–1496. https://doi.org/10.1001/jama.2020.19759
11. E. D. Bloom, D. Cadarette, J. P. Sevilla, Epidemics and economics, *International Monetary Fund. Communications Department*, **55** (2018), 46–48. https://doi.org/10.5089/9781484357415.022
12. M. Aniji, N. Kavitha, S. Balamuralitharan, Mathematical modeling of hepatitis b virus infection for antiviral therapy using lham, *Adv. Differ. Equ-Ny.*, **1** (2020), 1–19. https://doi.org/10.1186/s13662-020-02770-2
13. I. Zada, M. Naeem Jan, N. Ali, D. Alrowail, K. Sooppy Nisar, G. Zaman, Mathematical analysis of hepatitis b epidemic model with optimal control, *Adv. Differ. Equ-Ny.*, **1** (2021), 1–29. (https://doi.org/10.1186/s13662-021-03607-2).

14. S. Zhao, Z. Xu, Y. Lu, A mathematical model of hepatitis b virus transmission and its application for vaccination strategy in china, *Int. J. Epidemiol.*, **29** (2000), 744–752. https://doi.org/10.1093/ije/29.4.744

15. S. Means, M. A. Ali, H. Ho, J. Heffernan, Mathematical modeling for hepatitis b virus: Would spatial effects play a role and how to model it?, *Frontiers Physiol.*, **11** (2020), 146. https://doi.org/10.3389/fphys.2020.00146

16. Z. Khatun, M. S. Islam, U. Ghosh, Mathematical modeling of hepatitis b virus infection incorporating immune responses, *Sensors Int.*, **1** (2020), 100017. https://doi.org/10.1016/j.sintl.2020.100017

17. S. Zhang, Y. Zhou, The analysis and application of an hbv model, *Appl. Math. Model.*, **36** (2012), 1302–1312. https://doi.org/10.1016/j.apm.2011.07.087

18. S. A. Khan, K. Shah, P. Kumam, A. Seadawy, G. Zaman, Z. Shah, Study of mathematical model of hepatitis b under caputo-fabrizo derivative, *AIMS Math.,* **6** (2021), 195–209. https://doi.org/10.3934/math.2021013

19. Attaullah, M. Sohaib, Mathematical modeling and numerical simulation of HIV infection model, *Results Appl. Math.*, **100118** (2020), 1–11. https://doi.org/10.1016/j.rinam.2020.100118

20. S. Hussain, Z. Salleh, Continuous galerkin petrov time discretization scheme for the solutions of the Chen system, *J. Comput. Nonlin. Dyn.*, **10** (2015). https://doi.org/10.1115/1.4029714

21. S. Hussain, Numerical analysis of new class of higher order Galerkin time discretization schemes for nonstationary incompressible flow problems, Ph.D thesis, Der Fakultät Für Mathematik der Technischen Universität Dortmund Vorgelegt Von.

22. R. D. Attaullah, W. Weera, Galerkin time discretization scheme for the transmission dynamics of hiv infection with non-linear supply rate, *AIMS Math.*, **6** (2022), 11292–11310. https://doi.org/10.3934/math.2022630

23. F. Schieweck, A-stable discontinuous Galerkin-Petrov time discretization of higher order, *J. Numer. Math.*, **18** (2010), 25–57. https://doi.org/10.1515/JNUM.2010.002

24. S. Hussain, F. Schieweck, S. Turek, Higher order Galerkin time discretizations and fast multigrid solvers for the heat equation, *J. Numer. Math.*, **19** (2011), 41–61. https://doi.org/10.1515/JNUM.2011.003

25. S. Hussain, F. Schieweck, S. Turek, A note on accurate and efficient higher order Galerkin time stepping schemes for the nonstationary Stokes equations, *The Open Numerical Methods Journal*, **4** (2012) 35–45. https://doi.org/10.2174/1876389801204010035

26. Attaullah, R. Jan, S. Y zbasi, Dynamical behaviour of HIV infection with the influence of variable source term through galerkin method, *Chaos, Solitons and Fractals*, **152** (2021), 1–13. https://doi.org/10.1016/j.chaos.2021.111429

27. Attaullah, A. Jabeen, R. Jan, Solution of the HIV infection model with full logistic proliferation and variable source term using galerkin scheme, *Matrix Sci. Math. (MSMK)*, **4** (2020), 7. https://doi.org/10.26480/msmk.02.2020.37.43

28. T. Khan, G. Zaman, M. I. Chohan, The transmission dynamic and optimal control of acute and chronic hepatitis B, *J. Biol. Dynam.*, **11** (2017), 172–189. https://doi.org/10.1080/17513758.2016.1256441
29. C. O. Leary, Z. Hong, F. Zhang, M. Dawood, G. Smart, K. Kaita, et al., A mathematical model to study the effect of hepatitis b virus vaccine and antivirus treatment among the canadian inuit population, *Eur. J. Clin. Microbiol.*, **29** (2010), 63–72. https://doi.org/10.1007/s10096-009-0821-6
30. L. Zou, W. Zhang, S. Ruan, Modeling the transmission dynamics and control of hepatitis b virus in china, *J. Theor. Biol.*, **262** (2010), 330–338. https://doi.org/10.1016/j.jtbi.2009.09.035
31. S. Thornley, C. Bullen, M. Roberts, Hepatitis b in a high prevalence new zealand population: A mathematical model applied to infection control policy, *J. Theor. Biol.*, **254** (2008), 599–603. https://doi.org/10.1016/j.jtbi.2008.06.022
32. S. Hahné, M. Ramsay, K. Balogun, W. J. Edmunds, P. Mortimer, Incidence and routes of transmission of hepatitis b virus in england and wales, 1995–2000: Implications for immunisation policy, *J. Clin. Virol.*, **29** (2004), 211–220. https://doi.org/10.1016/j.jcv.2003.09.016
33. S. Hussain, F. Schieweck, S. Turek, Higher order Galerkin time discretizations and fast multigrid solvers for the heat equation, *J. Numer. Math.*, **19** (2011), 41–61. https://doi.org/10.1515/jnum.2011.003
34. S. Hussain, F. Schieweck, S. Turek, An efficient and stable finite element solver of higher order in space and time for nonstationary incompressible flow, Tech. rep., Fakultät für Mathematik, TU Dortmund, ergebnisberichte des Instituts für Angewandte Mathematik, **450** (2012). https://doi.org/10.1002/fld.3831
35. G. Matthies, F. Schieweck, Higher order variational time discretizations for nonlinear systems of ordinary differential equations, **23** (2011).
36. A. Aziz, P. Monk, Continuous finite elements in space and time for the heat equation, *Math. Comput.*, **52** (1989), 255–274. https://doi.org/10.1090/S0025-5718-1989-0983310-2
37. G. Matthies, F. Schieweck, Higher order variational time discretizations for nonlinear systems of ordinary differential equations, Technische Informationsbibliothek u. Universitatsbibliothek, 2011.
38. Attaullah, Zeeshan, M. T. Khan, S. Alyobi, M. F. Yassen, D. Prathumwan, A computational approach to a model for HIV and the immune system interaction, *Axioms*, **11** (10), 578. https://doi.org/10.3390/axioms11100578
39. W. Kutta, Beitrag zur naerungsweisen integration totaler differential gleichungen, *Z. Math. Phy.*, **46** (1901), 435–453.
40. J. Butcher, Numerical methods for ordinary differential equations, *Wiley, Hoboken, N. J.*, 2016.
41. G. Chen, T. Ueta, Yet another chaotic attractor, *Int. J. Bifurcat. Chaos*, **9** (1999), 1465–1466. https://doi.org/10.1142/S0218127499001024
42. Richard, L. Burden, J. D. Faires, Numerical analysis Ninth Edition.

43. Attaullah, S. Yuzbasi, S. Alyobi, M. F. Yassen, W. Weera, A Higher-Order Galerkin Time Discretization and Numerical Comparisons for Two Models of HIV Infection, Computational and Mathematical Methods in Medicine, Volume 2022, Article ID 3599827, 24 pages. https://doi.org/10.1155/2022/3599827

44. Attaullah, Khurshaid, A. Zeeshan, S. Alyobi, M. F. Yassen, D. Prathumwan, Computational Framework of the SVIR Epidemic Model with a Non-Linear Saturation Incidence Rate. Axioms 2022, 11, 651. https://doi.org/10.3390/axioms11110651

AIMS Press